ACS OMEGA

Open Access

http://pubs.acs.org/journal/acsodf

Article

Experimental Performance Evaluation and Optimization of a Weak Gel Deep-Profile Control System for Sandstone Reservoirs

Kazunori Abe,* Khwaja Naweed Seddiqi,* Jirui Hou, and Hikari Fujii

Cite This: *ACS Omega* 2024, 9, 7597−7608

Read Online

ACCESS | Metrics & More | Article Recommendations

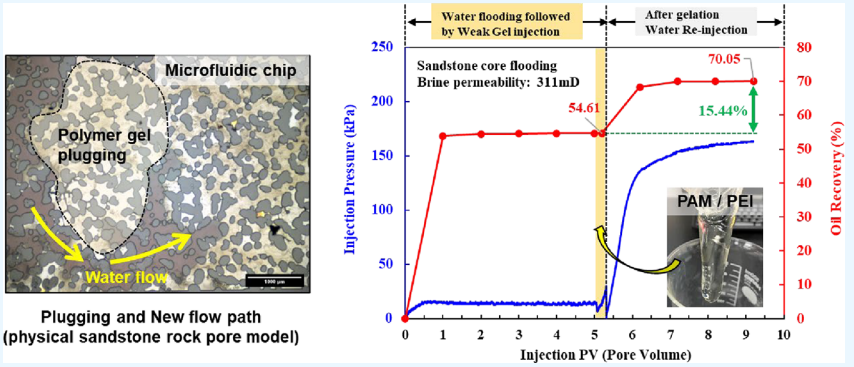

ABSTRACT: Globally, most oil fields use excessive water flooding to recover oil. By injection of water between wells, channels are created, which result in lower oil recovery. Water-plugging deep-profile control must be used to control the excessive water production from an oil reservoir. This laboratory study used sulfonated polyacrylamides with a molecular weight of 10.3−13.0 × 10^6 Da (FPAM) and polyethylenimine (PEI-600) to formulate a weak gel system to control excessive water production from deep formations. Using different FPAM and PEI-600 concentrations, the Sydansk bottle test approach was applied to evaluate the gelation time, strength, and stability of the weak gel. The weak gel concentration of 0.5 wt % FPAM and 0.4 wt % PEI-600 was confirmed for deep-profile control by this approach. The temperature and salt resistance of the selected weak gel system were evaluated using the same bottle test methodology. The gelation time depends on temperature: 5−7 days at <100 °C to 0.5 days >100 °C. Salinity >20,000 mg/L significantly affected the weak gel system's strength. By performing a viscometer test, the viscosity of the weak gel system at different times was evaluated, confirming the gelation time of the selected weak gel. Next, a microfluidic chip flooding test analyzed weak gel performance and plugging ability in porous media. This micromodel provided a visual analysis of the weak gel plug. Finally, a low- to medium-permeability sandstone core-flooding was conducted to determine the plugging rate of weak gel at the core scale, followed by an evaluation of the injection pressure, blocking effect, and oil recovery. According to the study, the selected weak gel has an extended gelation time with a significantly low viscosity, which affects its injectivity and can move from injection wells into deep formations. In the core-flooding test, the weak gel's blocking rate after 7 days of gelation time exceeded 90%.

1. INTRODUCTION

Oil industries worldwide depend greatly on oil fields and resources, and a major proportion of global economies depend directly on oil exploration and exploitation. As the world's most significant and critical energy resource, oil is essential for various public and private uses. Worldwide, the conservation of crude oil reserves is one of the most crucial components of macroeconomics and the energy sectors.[1] The standard rate of oil production decreases daily, and most of the world's giant oil reservoirs are in their secondary stage of production.[2−5] Consequently, enhanced oil recovery techniques are potential future solutions in the oil industry for sustaining production from oil reservoirs.[6]

In the late stage of water injection, a critical concern for the water flooding process is how to efficiently shut-in the high-permeability channels created by water flooding in the deep area of the layers and change the direction of injected water into the bypassed low-permeability regions. Decades of in-depth exploration of oil by water flooding method have resulted in

Received: September 3, 2023
Revised: January 23, 2024
Accepted: January 26, 2024
Published: February 8, 2024

widely spread residual oil mainly distributed in the deep interwell zone.[7]

A bulk gel system is used as a chemical flooding mechanism for excessive water production control. In this method, the in situ bulk gel is injected into the reservoir to block water channels.[8] Under specific conditions, the bulk gel system produces intermolecular cross-linking of the polymer and a cross-linker. Based on the cross-linking between molecules, the bulk gel has more effective viscoelastic characteristics and can be used to mitigate the effect of high-permeability layers or fractures in the formation to improve the macroscopic sweep efficiency.[6] Polymer gels are often used in mature reservoirs due to their good profile control capabilities, ease of production, and ability to reduce excessive permeability.[9] The low fluidity of polymer gel makes it only effective in strata within 10 m of the wellbore when multiscale pores coexist in the reservoir, which limits its profile control and displacement capability.[6]

Polymers with low concentration and slow-release cross-linkers could be mixed and injected into deep formation wells to develop the sweep efficiency, displace oil, and enhance deep-profile control. Since weak gels enhance molecular polymer migration and bulk gel profile control, these gels have become a focus of research.[10−15] Weak gel viscosity can range from 100 to 10,000 cP.[14] Sheng stated that weak gels have significant flow resistance but can flow, enabling their injection deep into reservoirs.[16] Similarly, Han referred to weak gels as flowing gel processes.[17] In addition to acting as oil displacement agents, weak gels also function as blocking agents, according to Song and Lu.[18,19] Shi-yi et al. reported that injection profiles can be adjusted, and oil displacement recovery can be increased by using weak gel flooding technology.[20] In contrast to using traditional gels or polymers for profile control, high-concentration gels solidify fast and are useful in blocking the wellbore vicinity.[21] Weak gels outperform conventional gels by exhibiting a comparatively high polymer and cross-linker concentration, short gel formation time, high gel strength, and high cost. As a result, conventional gels can only be used to adjust shallow reservoir permeability and not manage heterogeneity in deep reservoirs.[22] As opposed to conventional gels, weak gels inject a specific concentration of polymer and cross-linking agent into deep reservoirs using delayed cross-linking technology. This results in the formation of a polymer gel of specified strength in a high-permeability zone away from the injector, which then forces the fluid to move into a low-permeability zone with high oil saturation, expanding the sweep volume and improving oil displacement efficiency.[23,24]

Several gel systems have been developed for oil reservoirs with different conditions, including particle gels, gel agents that have excellent salt resistance, solvent−polymer weak gels, colloidal dispersion gels, and an ultrahigh molecular weight-hydrolyzed polyacrylamide (HPAM)/phenolic weak gel system,[23−27] which effectively expand the applicability and potential of weak gels. Furthermore, the combination of weak gels and microorganisms, as well as the CO_2−gel fracturing system in shale oil reservoirs, is a new trend.[28,29] However, the flow properties of weak gel systems in porous media are not fully understood. Additionally, the micromechanisms of oil displacement, achieved by reducing the relative permeability of the water phase in high-permeability channels and widening the water flooding swept area, remain unclear.

This paper evaluates the optimal formulation of a weak gel system that uses sulfonated polyacrylamides with a molecular weight of 10.3−13.0 × 10^6 Da with the commercial name of FLOPAM AN905 SH (hereafter referred to as FPAM) and polyethylenimine (PEI-600) for controlling excessive water production in a sandstone reservoir with high-water cut. Our methodology uses laboratory experiments that apply Sydansk bottle tests, and the gelation time, stability, and strength were evaluated. The properties of the selected weak gel system, such as temperature and salt resistance, were confirmed by the same method. Additionally, the viscosity of this weak gel system for deep-profile control was evaluated. For the conformance control and transportability of our formulated weak gel, a microfluidic chip flooding test was conducted with a physical rock structure model to evaluate the details of plugging ability in porous media,[30] which was followed by visualization analysis of the weak gel system. To understand the plugging performance of the weak gel at the core scale, a core-flooding test was applied to evaluate the weak gel system plugging effect and oil recovery at <60 °C.

2. EXPERIMENTAL SECTION

2.1. Materials and Equipment. The main agent for the weak gel is sulfonated polyacrylamide (FPAM), which is illustrated in Figure 1, and provided by SNF Water Science.

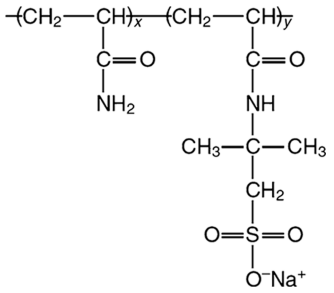

Figure 1. Sulfonated polyacrylamides (FPAM).

Other chemicals included the cross-linking agent, polyethylenimine, with an average molecular weight of 600 (PEI-600), thiourea (used for the deoxidation of brine), and NaCl (used to make a brine with a salinity of 0.5 wt % NaCl), which were acquired from Fujifilm Wako Chemical Corporation, Japan. Berea Buff sandstone (brine permeability 146−409 mD) prepared from Kocurek Industries, Inc. Texas, USA, was used in the core-flooding test.

Major laboratory equipment included a DV2T Brookfield viscometer (Brookfield Engineering Laboratories, Inc., Middleboro, MA, USA), an advection pump, and a VINCI SRP350 apparatus (VINCI Technologies, Nanterre, France), which was used for the core-flooding test. In the Micronit microfluidic model (Micronit, Enschede, Netherlands), a simulated sandstone chip was used for the flooding test. A stirrer, a precision balance (0.001 g), and a constant temperature chamber were also included in the lab test equipment.

2.2. Methods. *2.2.1. Formula Optimization of the Weak Gel System.* The weak gel solution was prepared from low molecular weight FPAM and cross-linking agent PEI-600. The steps in this experiment are as follows.

(1) A fixed volume of water was added to a 500 mL beaker, and the deoxidant (0.005 wt %) and the dosage of salt were mixed in.
(2) The dosage of the main ingredient (FPAM) was calculated, weighed accurately using the balance, added to the beaker, and stirred at 600 rpm for the first 10 min,

https://doi.org/10.1021/acsomega.3c10244
ACS Omega 2024, 9, 7597−7608

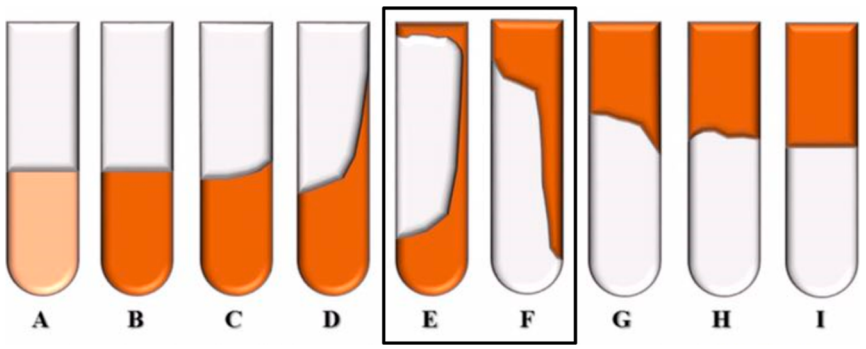

Figure 2. Schematic guide to different gel strengths and associated code:[11] (A) no detectable continuous gel formed; (B) highly flowing gel; (C) flowing gel; (D) moderately flowing gel; (E) gel with minimal flow; (F) highly deformable nonflowing gel; (G) moderately deformable nonflowing gel; (H) slightly deformable nonflowing gel; and (I) rigid gel.

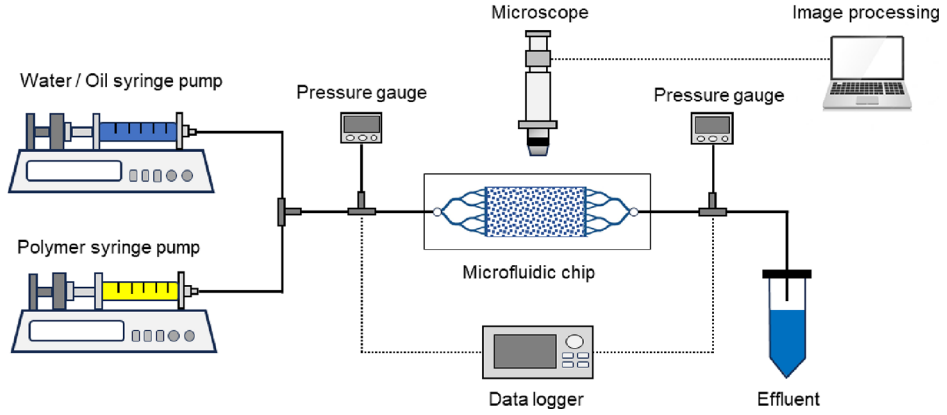

Figure 3. Schematic diagram of microfluidic flooding test model.

followed by 400 rpm for 4 h.[31] Afterward, the solution was aged for 24 h.

(3) The amount of cross-linking agent (PEI-600) was calculated, weighed accurately, added to the beaker, and then stirred for 20 min at 400 rpm to ensure proper dissolution.

(4) The prepared solution was poured into a glass medicine bottle and placed in the thermostatic chamber. The gel state of the solution was observed, and a record was kept for the gelation time.

The content of the main agent (FPAM) was fixed at 0.4, 0.5, and 0.6 wt %, and the quantity of the cross-linker (PEI-600) was changed from 0.3 to 0.6 wt %. A 300 mL volume of FPAM solution was prepared, and the designated amount of PEI-600 was poured into 50 mL of the prepared solution, followed by stirring for 20 min. Afterward, 10 mL of the stirred mixture was poured into a glass medicine bottle and placed in the thermostatic chamber. The gelation time and gel strength of the weak gel system under the specified concentrations and dosages of PEI-600 were measured by using the Sydansk bottle test. All experiments were duplicated to ensure minimal errors. Figure 2 shows the guide used to estimate gel strength.[11] The targeted weak gel strength for profile control in this study is codes E−F (black line in Figure 2).

2.2.2. Salt Resistance Evaluation of the Weak Gel System. Brine represented by 0.1, 0.5, 1.0, 2.0, and 3.0 wt % salinities was used to evaluate the system's salinity resistance. In this test, the content of the main agent (FPAM) and cross-linker (PEI-600) was fixed at 0.5 and 0.4 wt %, respectively. The gelation time and gel strength of the weak gel system were measured as described in Section 2.2.1.

2.2.3. Temperature Resistance Evaluation of the Weak Gel System. To evaluate the gelling time and viscosity at variable temperature, the selected weak gel system, formulated with 0.5 wt % FPAM and 0.4 wt % PEI-600, was stored in a temperature chamber at different temperatures: 60, 80, 100, and 120 °C. Again, the gelation time and gel strength of the weak gel system were measured as described in Section 2.2.1.

2.2.4. Viscosity Evaluation Experiment of the Weak Gel System. After formulating the selected weak gel, it was used for viscosity evaluation; the steps in this experiment are as follows.

(1) From the prepared weak gel, a small amount of the solution was taken to measure the liquid viscosity using the viscometer.

(2) The remaining solution was placed in a constant temperature chamber (60 °C) and retrieved periodically to measure the viscosity.

(3) After the gel formed, its viscosity was measured.

2.2.4.1. Experimental Methods. The DV2T Brookfield viscometer was used to measure viscosity. Specifically, 300 mL of the weak gel solution consisting of FPAM (0.5 wt %) and cross-linking agent PEI-600 (0.4 wt %) was prepared and placed in the thermostatic chamber. Initially, and then at 1, 2, 3, 4, 5, 6, 7, 12, and 30 days, the liquid was retrieved to measure its viscosity under the various conditions described above. Finally, the system's adhesiveness performance was recorded and evaluated.

https://doi.org/10.1021/acsomega.3c10244
ACS Omega 2024, 9, 7597−7608

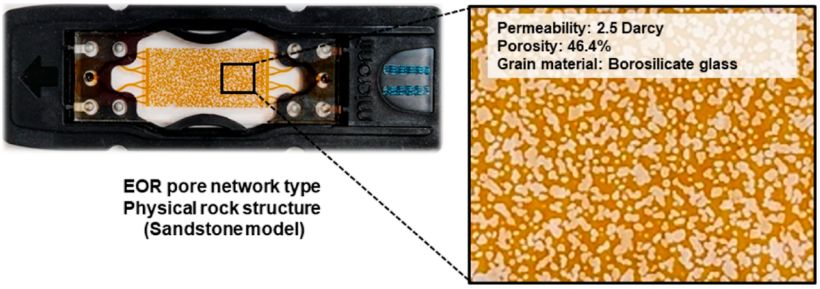

Figure 4. Microscopy imaging position on the microfluidic chip.

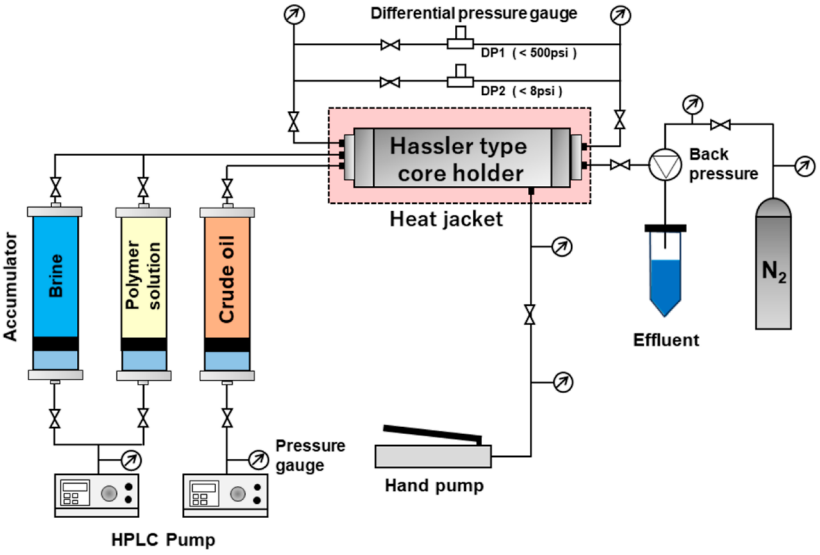

Figure 5. Schematic diagram of the gel-blocking experiment apparatus.

2.2.5. Flooding Test and Imaging Procedure in the Microfluidic Chip. 2.2.5.1. Experimental Conditions. The plugging capability of the weak gel in a sandstone-based simulation was evaluated visually using a microfluidic chip model. The schematic diagram of the microfluidic flooding model (Figure 3) includes syringe pumps (YMC, YSP-101), a chip holder, a microscope device (Shodensha, NSH130CSLT), and tools for the imaging process. As shown in Figure 4, images covering a specific area in the chip model can be examined and analyzed. In this test, the simulated formation water is first injected into the chip until it is fully saturated. For the aging process, 0.1 PV-defined weak gel was injected and placed in the thermostatic chamber for 1 week. Following the aging process, the brine is reinjected to evaluate the blocking rate after a weak gel injection. The steps of this experiment are as follows.

(1) About 5 mL of the brine was drawn into a syringe that was joined to a tube connector and tube. To prevent the gas in the syringe from entering the microchannel model and adversely affecting the results, the syringe body was gently tapped by hand to expel any gas in the syringe and tube.
(2) The syringe was attached to the pump, and the pump was operated until the 0.1 PV was injected into the microfluidic chip.
(3) The microchannel model was placed in the microchannel model holder, the holder was closed, and the tube and the microchannel model were connected.
(4) To gather images of the microchannel model, the position of the microchannel model was finely adjusted using the dial on the microscope pedestal while checking the microscope image displayed on the microscope software (Machine Vision Software—MVS, be Vision, Brescia, Italy).
(5) The flow rate of the pump was set at 0.1 μL/min, and the pump was activated.
(6) During the flooding test, microscope images and videos were taken using the MVS microscope software. Additionally, to prevent overexposure in the image, the illuminance was maintained at a moderate setting.

2.2.6. Weak Gel Core-Flooding Test Method. 2.2.6.1. Experimental Methods and Procedures. Berea Buff sandstone core samples with the range of 150−450 mD permeabilities were used for deep-profile core-flooding control. There were two scenarios investigated: the first scenario was to evaluate the selected weak gel blocking rate. The core samples were saturated only with brine with no oil recovery treated as a base model, while the second scenario included the oil recovery effect. In both scenarios, the core sample was degassed and saturated with brine for 24 h. The brine was then injected into the core until the injection pressure became constant (Δp_1). In the first scenario, the next 0.15 PV prepared solution was injected into the core. The core was removed from the core holder and placed in the thermostatic chamber (60 °C) for 1 week to allow the prepared solution to become a weak gel. The core sample was relocated to the core holder, and brine was reinjected, after which the pressure (Δp_2) was again recorded. The pressure difference before weak gel injection and after weak gel injection was calculated. The change in the injection pressure through time

https://doi.org/10.1021/acsomega.3c10244
ACS Omega 2024, 9, 7597−7608

Table 1. Aging Core Sample Properties Used for Core Blocking Rate and Oil Recovery by Flooding Test

core ID	diameter (mm)	length (mm)	brine permeability (mD)	pore volume (cc)	porosity (%)	experiment
BB_1	37.67	76.12	409.96	18.87	22.24	plugging rate test
BB_2	37.93	75.99	324.86	19.31	22.49	
BB_3	38.01	76.08	158.87	17.36	20.10	
BB_4	38.11	75.95	311.07	19.41	22.40	oil recovery evaluation
BB_5	38.19	76.16	146.97	17.54	20.10	

was recorded, and the blocking rate of the weak gel system was calculated using eq 1

$$\text{Blocking rate}\ (\%) = \frac{\Delta p_2 - \Delta p_1}{\Delta p_2} \times 100\% \quad (1)$$

During the flooding test, the flow rate is constant at 0.4 mL/min. The specific experimental steps are as follows.

(1) The experimental device was installed according to the schematic diagram (Figure 5), and the Berea sandstone core sample was saturated with brine. The pore volume, porosity, brine permeability, and injection pressure were measured during the brine injection.
(2) The weak gel solution was injected into the core sample, and it was placed in the thermostatic chamber for 1 week. It was then relocated to the core holder, and the brine was reinjected; the injection pressure and relevant data were recorded and the plugging rate was calculated.

In the second scenario, the brine was injected to calculate its permeability, then the oil was injected for oil saturation, and the core was aged by crude oil for 3 weeks. In this study, the degassed light crude oil with a density of 0.86 g/cm^3 (API gravity 35°) and a viscosity of approximately 7.7 cP at 22 °C was used. The brine was then injected as the primary recovery, followed by a 0.15 PV weak gel injection for conformance control. The procedure is reset in the same way as described earlier. It was possible to compare the oil recovery rate and injection pressure before and after the selected weak gel conformance control treatment. Table 1 lists the details of the core samples used for the plugging effect and oil recovery by a weak gel.

3. RESULTS AND DISCUSSION

The temperature and salt resistances of the formulated weak gel system were evaluated using the Sydansk bottle test method, which is a simple and effective approach to assessing the performance of a weak gel.[11] The weak gel viscosity was also evaluated by the viscometer test method for 7 days before and 2 days after gelation, and its result was offered. Finally, in the last part of this paper, the performance of weak gel-blocking ability was evaluated by microfluidic chip flooding and a core-flooding test method. The pH of the weak gel system employed in this study was set within the range of 5−7.

3.1. Optimal Formulation of Weak Gel System Result.

Optimization experiments focused on the gelation time and strength of the weak gel system to optimize the formulation. The aging performance of the selected weak gel (sample B-2) for the deep-profile control was observed, and the experimental results are shown in Figure 6 and Tables 2−4. The gel-forming time of the system was prolonged significantly when the cross-linking agent fixed at 0.3 wt %, and there was negligible effect on the gel strength. When the cross-linking agent content was increased, the gel strength of the system was enhanced, reaching the maximum strength E. We conclude that the performance of the weak gel system meets the requirements when the cross-linking agent is 0.4 wt % at 60 °C. Figure 7 shows the effect of the cross-linker (PEI-600) concentration on the gelation time.

Figure 6. Aging performance of the selected weak gel (samples B-2) for the deep-profile control.

Table 2. Aging Performance of the Weak Gel at 60 °C with FPAM Concentration at 0.4 wt %

no.	cross-linking agent (PEI-600, wt %)	gelation performance (days)				
		5	7	10	30	75
A-1	0.3	B	D	E	E	F
A-2	0.4	B	D	E	F	-
A-3	0.5	C	D	E	F	F
A-4	0.6	C	D	E	F	F

Table 3. Aging Performance of the Weak Gel at 60 °C with FPAM Concentration at 0.5 wt %

no.	cross-linking agent (PEI-600, wt %)	gelation performance (days)				
		5	7	10	30	75
B-1	0.3	D	E	F	F	F
B-2	0.4	E	F	F	F	F
B-3	0.5	D	F	G	G	G
B-4	0.6	E	F	F	F	F

The cross-linking mechanism governing the development of the weak gel involves a transamidation reaction. Specifically, within this process, FPAM, featuring amide functional groups, undergoes a chemical reaction with PEI-600, which is characterized by amine functionalities. This interaction leads to the formation of a new amide structure, constituting a key step in the establishment of a weak gel network. The transamidation

https://doi.org/10.1021/acsomega.3c10244
ACS Omega 2024, 9, 7597−7608

Table 4. Aging Performance of the Weak Gel at 60 °C with FPAM Concentration at 0.6 wt %

no.	cross-linking agent (PEI-600, wt %)	gelation performance (days)				
		5	7	10	30	75
C-1	0.3	D	F	F	G	G
C-2	0.4	E	F	F	G	H
C-3	0.5	E	F	F	G	G
C-4	0.6	E	F	F	G	H

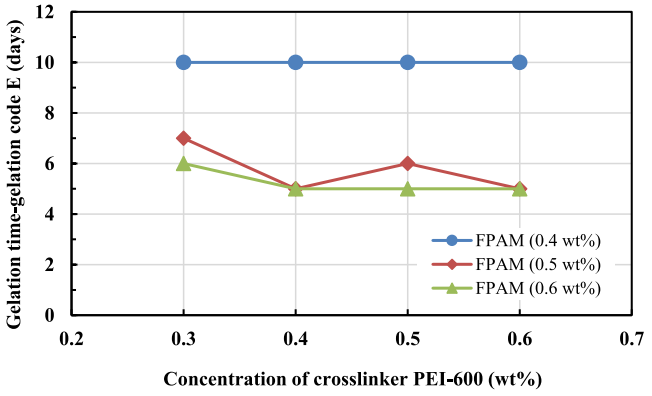

Figure 7. Effect of the cross-linker (PEI-600) concentration on the gelation time.

Table 5. Salt Resistance Test Results for the Weak Gel at 60 °C with FPAM 0.5 wt % and PEI 0.4 wt %

no.	NaCl concentration in brine (wt %)	gelation performance (days)						
		3	4	5	6	7	8	38
1	0.1	D	D	E	E	F	F	F
2	0.5	D	D	E	F	F	F	F
3	1	C	C	D	E	E	E	F
4	2	B	B	C	C	D	D	E
5	3	B	B	C	C	C	C	D

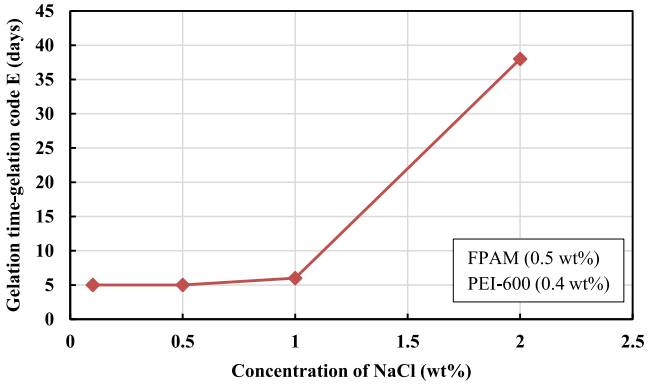

Figure 8. Effect of the NaCl concentration on the gelation time.

reaction, at the molecular level, contributes to the structural integrity and viscoelastic properties of the resultant weak gel, providing essential insights into the controlled design and application of such materials in various contexts, particularly in the realm of conformance control within porous media.[32−35]

3.2. Evaluation of the Salt Resistance of the Weak Gel System Result. The Sydansk bottle test method was applied to evaluate the salt resistance of the weak gel system. The brine with salinities 1000, 5000, 10,000, 20,000, and 30,000 mg/L

Table 6. Evaluation Results for the Temperature Resistance Performance of the Weak Gel System with FPAM 0.5 wt %, PEI-600 0.4 wt %, and 0.5 wt % Salinity

no.	temperature (°C)	gelation performance (days)							
-	-	1	2	3	4	5	7	10	34
1	60	B	B	C	C	D	E	F	F
2	80	B	C	D	D	E	E	F	F
3	100	B	D	E	F	F	F	F	F
4	120	G	G	G	G	G	G	-	-

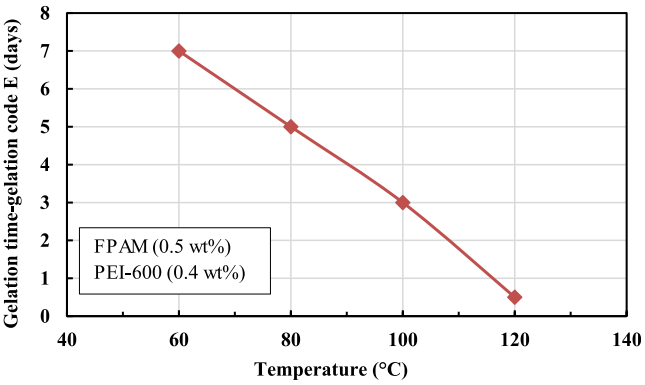

Figure 9. Effect of temperature on the gelation time.

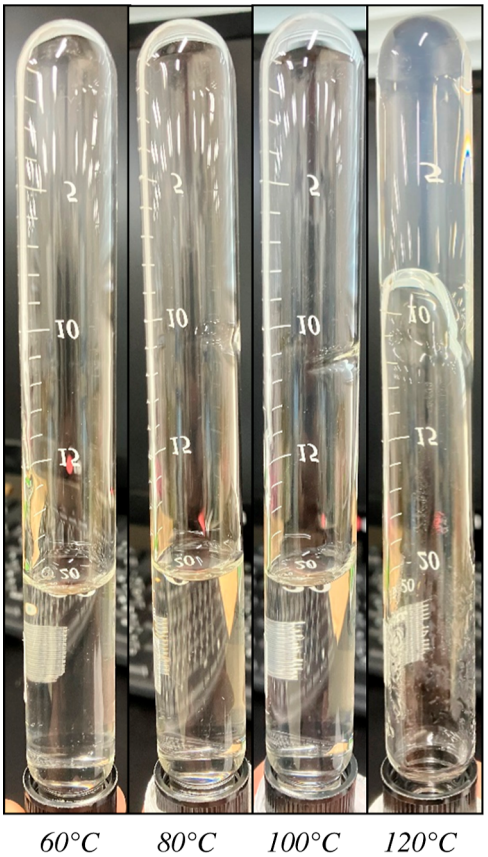

Figure 10. Weak gel performance after 1 day of aging under different temperatures.

NaCl with 0.5 wt % FPAM and 0.4 wt % PEI-600 were used to investigate the formulated weak gel system's salt resistance. Table 5 presents the results of the salt tolerance evaluation for the weak gel system exposed to variable salinity conditions.

https://doi.org/10.1021/acsomega.3c10244
ACS Omega 2024, 9, 7597−7608

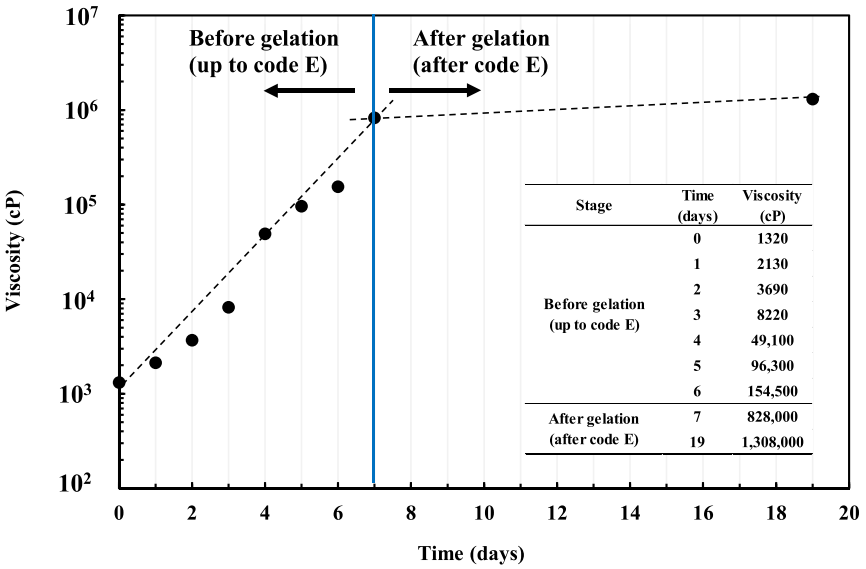

Figure 11. Viscosity measurement results for FPAM 0.5 wt % and PEI-600 0.4 wt %.

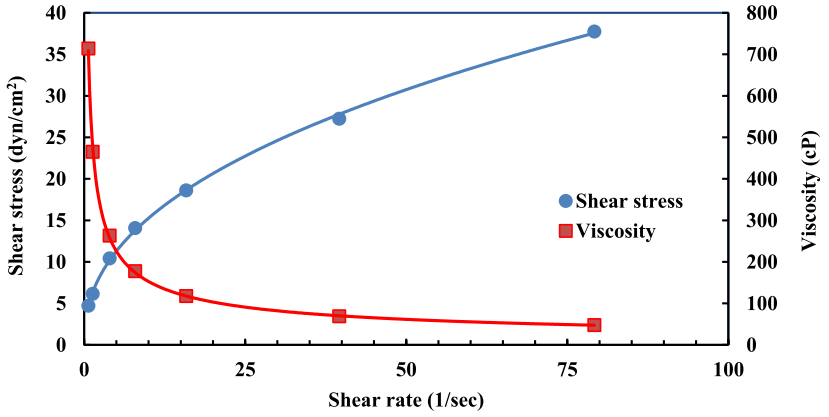

Figure 12. Shear stress vs shear rate for the confirmed weak gel before aging time.

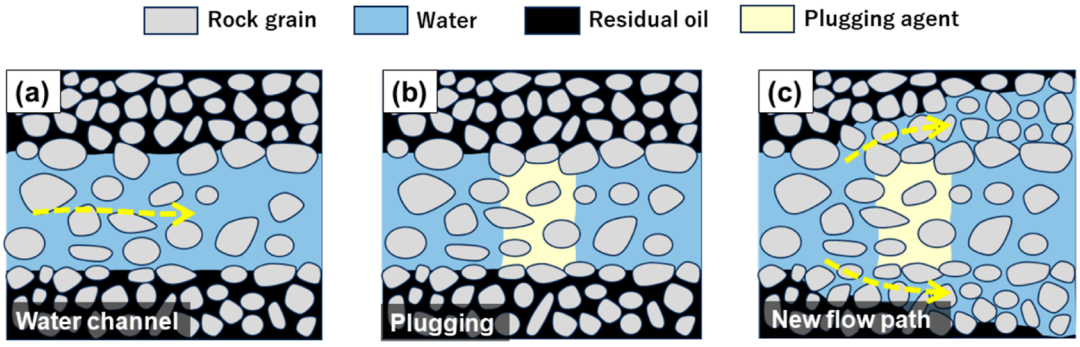

Figure 13. Using chemicals to control fluid flow and improve oil recovery. The process involves (a) injecting water which creates a path, (b) injecting a plugging agent to block the flow, and (c) changing the water flow path to force the remaining oil toward the outlet, resulting in improved oil recovery.[36]

Figure 8 shows the effect of the NaCl concentration on the gelation time in the same weak gel system.

Relative to the initial salinity of 5000 mg/L, Table 5 shows that with the increase in the salinity of the brine, the strength of the weak gel system decreases. The brine salinity considerably influences the weak gel strength. When the brine salinity was >20,000 mg/L, the viscosity of the weak gel decreased sharply, and the gel strength was less than D. The 0.5 wt % FPAM and 0.4 wt % PEI-600 weak gel system has good salt tolerance and can maintain its resistance within brine salinities that are <20,000 mg/L.

3.3. Weak Gel System Temperature Resistance Evaluation Result. The Sydansk bottle test method was used to evaluate the temperature resistance of the weak gel system. The simulated temperatures were set at 60, 80, 100, and 120 °C as shown in Table 6. Starting at 60 °C, a weak gel's strength increases with temperature and then remains stable at high temperatures, as shown in the table. As the temperature rises, the

https://doi.org/10.1021/acsomega.3c10244
ACS Omega 2024, 9, 7597−7608

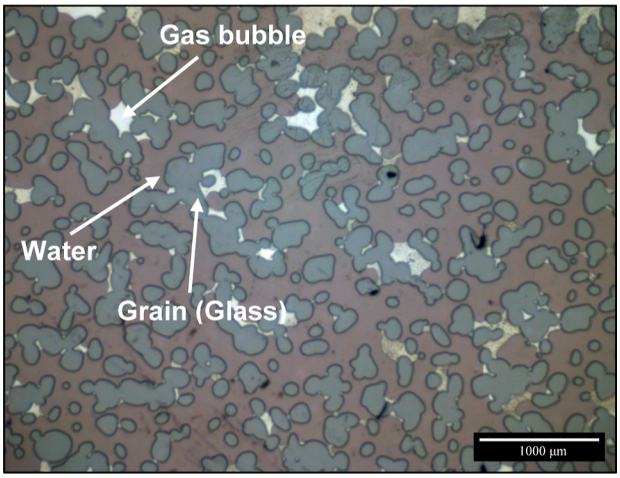

Figure 14. Distribution of water before the weak gel injection. The white collars indicate gas bubbles.

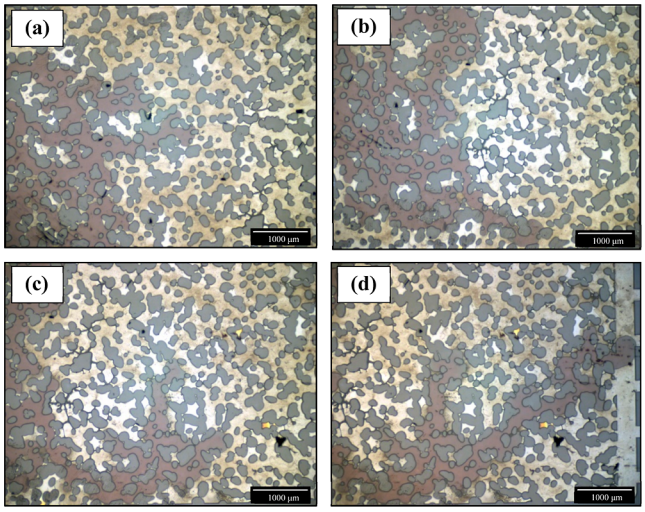

Figure 15. Outcome of the microfluidic chip's weak gel plugging process: (a) influx of water into the chip; (b) flow path alteration due to weak gel blockage; (c) emergence of a new flow pathway for fluid (brine); and (d) discharge of brine through the outlet via the newly established flow pathway.

gelation time decreased; at the high temperature of 120 °C, the gelation time is less than 12 h, and the gel strength is G. However, the degradation time is short at temperatures >100 °C, and the gel degraded after 10 days. When the temperature exceeds 100 °C, the gel performance and its strength increase significantly. Figure 9 shows the effect of variable temperature on the weak gel system's gelation time. Comprehensively, the 0.5 wt % FPAM and 0.4 wt % PEI-600 weak gel system has favorable temperature resistance and can maintain good stability at <100 °C. Figure 10 illustrates the weak gel bottle samples at selected temperatures after 1 day. In this figure, the strength of G can be observed in the high-temperature samples.

3.4. Viscosity Evaluation of Weak Gel System Result. Evaluation of the adhesive performance of the weak gel system was studied to determine the strength of the gel. The results are listed in Figure 11. Before gelation, the viscosity of the solution started from 1320 cP. The overall viscosity was low, indicating favorable weak gel injectability. After gelation, the viscosity of the gel was several orders of magnitude greater than that before

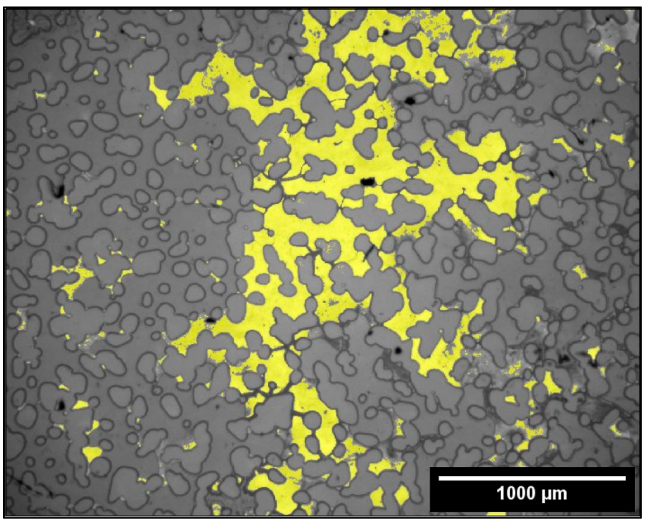

Figure 16. Distribution of water after gel (yellow) injection into the microfluidic chip.

Table 7. Blocking Rate Results for Weak Gel Obtained through the Core-Flooding Test

core ID	permeability (mD)	breakthrough pressure (kPa) wait for 1 week	blocking rate (%) wait for 1 week
BB_1	409	21.77	98.33
BB_2	324	35.30	95.38
BB_3	158	99.28	97.02
core ID	permeability (mD)	breakthrough pressure (kPa) wait for 4 weeks	blocking rate (%) wait for 4 weeks
BB_1	409	17.89	96.81
BB_2	324	19.69	91.72
BB_3	158	35.16	95.30

gelation, with the maximum reaching 828,000 cP. The shear stress versus shear rate of the confirmed weak gel before aging time is indicated in Figure 12. Comprehensively, the weak gel system solution has good injectability, and the strength of the gel meets the plugging requirements.

3.5. Evaluation of the Plugging Performance of the Weak Gel System—Microfluidic Chip Result. By using various gel and foam systems together with chemical agents, we can control water flow paths in porous media. As shown in Figure 13a, injected water does not affect the oil displacement. However, the water flow is blocked after introducing a chemical agent such as a gel or foam, as can be seen in Figure 13b. In Figure 13c, the chemical agent blocks the water flow path, allowing more oil to be displaced toward the outlet. The weak gel described in this paper has significant potential for application as a chemical agent since it can block the water flow path and improve the efficiency of water injection sweeps in oil reservoirs. Owing to their short gelation time, chemical agents such as starch gels cannot travel the long distance required to block the water channels. However, in this research, a weak gel with a long gelation time and sufficient blocking strength is introduced.

The weak gel plugging ability in a sandstone chip model is visually evaluated in this section and is illustrated in Figures 14−16. Figure 14 shows a relatively weak heterogeneity in the microscopic pore of the chip model, and the particle size distribution is relatively uniform. The brine is regularly distributed in the pore structure of the chip. As explained in

https://doi.org/10.1021/acsomega.3c10244
ACS Omega 2024, 9, 7597−7608

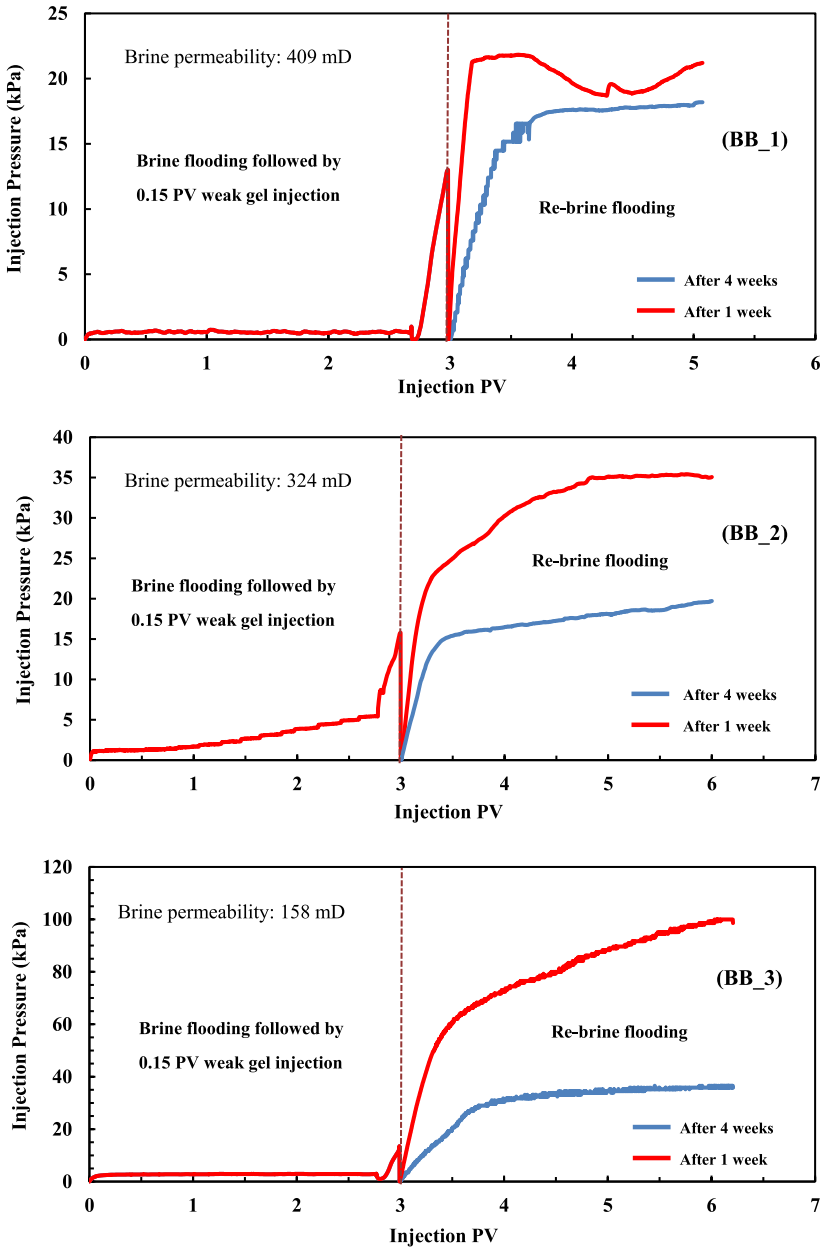

Figure 17. Comparison of injection pressure and breakthrough curves of BB_1, BB_2, and BB_3 core samples by selected weak gel after 1 and 4 weeks aging.

the methodology of the test, after evaluating water distribution, the weak gel is injected to assist its blocking ability and profile control. The microchip model is stored in the thermostatic chamber for 1 week to age, and then water is injected to distinguish water and gel particles. As observed in Figure 15a, the water moves forward and occupies channels, but it is stopped by the weak gel (Figure 15b), and it changes its flow path (Figure 15c). Figure 15d clearly shows the change in the brine flow path due to weak gel-blocking. Brine can then be produced through the outlet (Figure 15d). Figure 16 illustrates the final condition of the weak gel-blocking ability after water distribution; apparently, nearly >95% of the flow path is blocked.

3.6. Evaluation of the Plugging Performance of the Weak Gel System—Sandstone Core-Flooding Test Result. The performance of the plugging and oil recovery of the system was evaluated by recording the pressure changes and oil production through 7 days of gelation after injection of the weak gel. The test results at 60 °C are shown in Table 7. The injection pressure kept increasing steadily through time. When the permeability decreases, the injection pressure increases greatly. The outstanding performance of the selected weak gel plugging ability is also observed.

More test results at 60 °C are also shown in Figures 17 and 18. The injection pressure increases slowly and steadily with time, following initiation. When the permeability decreases from 409 to 158 mD, the injection pressure increases, and the effect of permeability changes is obvious, indicating that the injection performance of the weak gel system is related to the rock porosity; the greater the permeability, the better its injection performance, and selectivity is improved when it is easier to block the dominant channel.

After the mixture waited 7 days, the blocking performance of the weak gel was tested by brine flooding. Core sample BB_1 in Figure 17 shows that in the front stage of brine flooding, affected

https://doi.org/10.1021/acsomega.3c10244
ACS Omega 2024, 9, 7597−7608

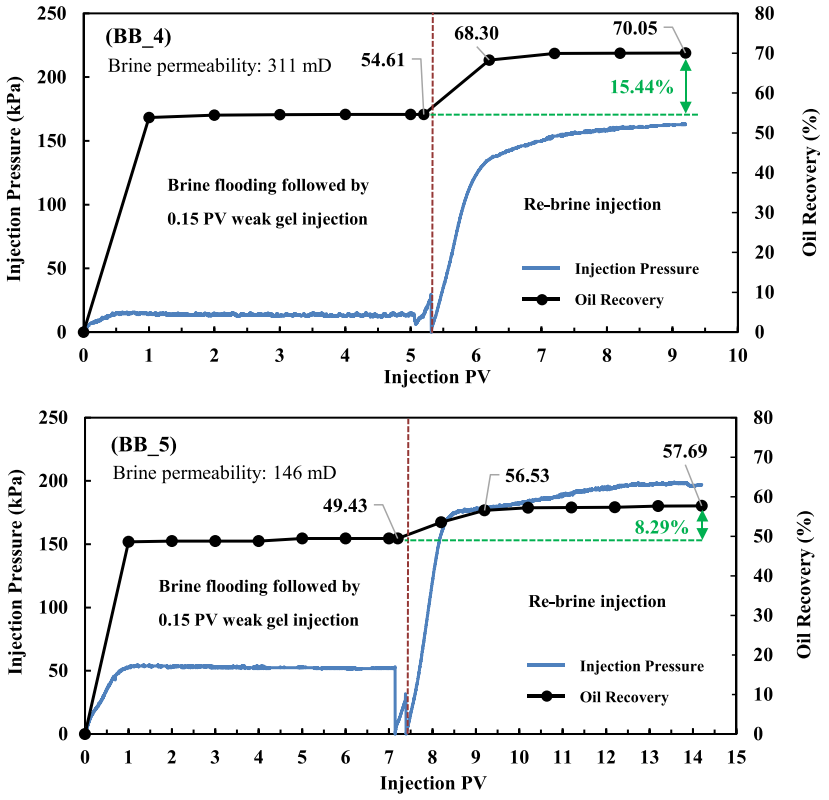

Figure 18. Oil recovery and injection pressure of BB_4 and BB_5 core samples by selected weak gel after 1 week of aging.

by the weak gel blockage, the pressure rises rapidly, reaches the maximum breakthrough pressure, and then falls to a certain stable pressure. However, the pressure continued increasing in the other samples, BB_2 and BB_3. As the core permeability decreases, the breakthrough pressure after the system is plugged increases significantly, and accordingly, the plugging rate increases slightly.

Generally, the weak gel system has strength and a blocking effect after 7 days of gelling. Under low permeability, the plugging breakthrough pressure reached 99.28 kPa, and the blocking strength was high. Overall, the plugging rate for the weak gel system reached more than 95% after 7 days of gelation at 60 °C.

The longer the waiting time, the more observable the effect of the temperature on the dehydration of the weak gel sample, resulting in a decrease in its strength. With increasing permeability, the breakthrough pressure decreased from 99.28 to 21.77 kPa. A graphical comparison of injection pressure and breakthrough curves by selected weak gel after 1 and 4 weeks is shown in Figure 17. From the perspective of the change in the plugging rate, breakthrough pressure increased slightly as the permeability became larger.

Figure 18 depicts the second scenario, which consists of the oil recovery and injection pressure results from two distinct permeability core samples, BB_4 (311 mD) and BB_5 (146 mD). The oil recovery rate of the sample with a higher permeability (BB_4) following conformance control by the selected weak gel is 15.4%, which is higher than that of the BB_5 core sample. The selected weak gel effect on pore plugging in sample BB_4 is greater, which may account for the higher rate of oil recovery compared to the BB_5 core sample.

Because the initial viscosity of the weak gel solution is low, the weak gel first penetrates a layer of high permeability at the beginning of the injection, resulting in low percolation resistance. The weak gel can remain in the pore throat of the high-permeability layer, increasing the percolation resistance of the weak gel agent moving through the region. The weak gel agent that was injected afterward begins to reach the other regions of the high- and medium-permeability layers.

When the weak gel begins to gel in the core, it creates an improved blocking ability in the high-permeability layer, causing the injection pressure to rise. Under increasing injection pressure, the injected water enters the medium- and low-permeability layers, achieving the goal of volume expansion. The weak gel enters the high-permeability layer preferentially, lowering the flow rate within the high-permeability layer and driving the injected water flow into the medium- and low-permeability layers, thus decreasing the volume of weak gel entering the low-permeability layer. As a result, the high- and low-permeability layers coincide as closely as feasible. The weak gel begins to gel as it enters the middle of the throat. At this point, the weak gel aggregates expand with water, strengthening the weak gel-blocking effect and driving injected water into the lower permeability layer.

Following injection of the weak gel, most of the oil in the large pores of the high-permeability layer has been washed out, and the residual oil is primarily distributed in the small pores. The weak gel solution cannot enter the narrow pores due to the polymer's massive molecular clusters. Under the same injection pressure conditions, the injected water can enter the small pore throat, so that the weak gel cannot easily reach and displace the microscopic residual oil.

4. CONCLUSIONS

The optimization of the weak gel system was meticulously conducted, focusing on key indices of gel formation, specifically,

https://doi.org/10.1021/acsomega.3c10244
ACS Omega 2024, 9, 7597−7608

the gelation time and strength. Subsequent to the optimization process, an adhesiveness evaluation experiment was conducted using the refined formula. Additionally, a dynamic sealing evaluation experiment was undertaken to comprehensively assess the system's performance. The significant findings and conclusions derived from these experiments are outlined below.

1. At an operational temperature of 60 °C, the optimized weak gel system formula achieved optimal parameters with a composition of 0.5 wt % FPAM concentration and 0.4 wt % PEI-600 concentration. The gelation process was observed over 7 days, resulting in a gelation strength denoted as F, as determined through the Sydansk bottle test approach. Notably, this optimized formula displayed a minimal viscosity of 1320 cP, ensuring favorable injectability pregelation. Subsequent to gelation, the viscosity significantly increased to 828,000 cP, highlighting the robust blocking strength characteristic of the weak gel.
2. The dynamic evaluation test results, specifically focusing on the system's plugging performance, demonstrated that even after 30 days of gelation at 60 °C, the modified weak gel system maintained a plugging rate exceeding 90%. This sustained effectiveness underscores the long-term stability and plugging capabilities of the optimized weak gel.
3. Following the application of a weak gel deep-profile control treatment on sandstone core samples with permeabilities ranging from 146 to 311 mD, a confirmed oil recovery rate within the range of 8.29−15.44% was achieved. These outcomes substantiate the practical efficacy of the weak gel in enhancing oil recovery within diverse sandstone reservoirs with varying permeabilities.

AUTHOR INFORMATION

Corresponding Authors

Kazunori Abe − *Department of Earth Resource Engineering and Environmental Science, Akita University, Graduate School of International Resource Sciences, Akita 010-8502, Japan;* orcid.org/0000-0001-9781-2416; Email: abe@mine.akita-u.ac.jp

Khwaja Naweed Seddiqi − *Center for Regional Revitalization in Research and Education, Akita University, Akita 010-8502, Japan;* orcid.org/0000-0003-3871-6445; Email: naweed.cedeqe@gmail.com

Authors

Jirui Hou − *The Unconventional Oil and Gas Institute, Changping, China University of Petroleum-Beijing, Beijing 102249, China*

Hikari Fujii − *Graduate School of International Resource Sciences, Department of Earth Resource Engineering and Environmental Science, Akita University, Akita 010-8502, Japan*

Complete contact information is available at: https://pubs.acs.org/10.1021/acsomega.3c10244

Notes

The authors declare no competing financial interest.

ACKNOWLEDGMENTS

This research was supported by JSPS KAKENHI grant number JP21K04959.

NOMENCLATURE

Δp_1	injection pressure before gel injection
Δp_2	injection pressure after gel injection
FLOPAM AN905 SH	commercial name of sulfonated polyacrylamides
PEI	polyethylenimine

REFERENCES

(1) Khojastehmehr, M.; Madani, M.; Daryasafar, A. Screening of enhanced oil recovery techniques for Iranian oil reservoirs using TOPSIS algorithm. *Energy Rep.* **2019**, *5*, 529−544.

(2) Höök, M.; Xu, T.; Xiongqi, P.; Aleklett, K. Development journey and outlook of Chinese giant oilfields. *Pet. Explor. Dev.* **2010**, *37* (2), 237−249.

(3) Song, W.; Yang, C.; Han, D.; Qu, Z.; Wang, B.; Jia, W. Alkaline-surfactant-polymer combination flooding for improving recovery of the oil with high acid value. *International Meeting on Petroleum Engineering*; OnePetro, 1995.

(4) Elaf, R.; Ben Ali, A.; Saad, M.; Hussein, I. A.; Bai, B. Development of eco-friendly chitosan-g-polyacrylamide preformed particle gel for conformance control in high-temperature and high-salinity reservoirs. *Geoenergy Sci. Eng.* **2023**, *230*, 212136.

(5) Sun, F.; Lin, M.; Dong, Z.; Zhu, D.; Wang, S. L.; Yang, J. Effect of composition of HPAM/chromium (III) acetate gels on delayed gelation time. *J. Dispersion Sci. Technol.* **2016**, *37* (6), 753−759.

(6) Bai, B.; Zhou, J.; Yin, M. A comprehensive review of polyacrylamide polymer gels for conformance control. *Pet. Explor. Dev.* **2015**, *42* (4), 525−532.

(7) Liu, Y.; Xiong, C.; Luo, J. Studies on indepth fluid diverting in oil reservoirs at high water cut stages. *Oilfield Chem.* **2006**, *23*, 248−251.

(8) Zaltoun, A.; Kohler, N.; Guerrinl, Y. Improved polyacrylamide treatments for water control in producing wells. *J. Pet. Technol.* **1991**, *43* (07), 862−867.

(9) Salehi, M. B.; Soleimanian, M.; Moghadam, A. M. Examination of disproportionate permeability reduction mechanism on rupture of hydrogels performance. *Colloids Surf., A* **2019**, *560*, 1−8.

(10) Smith, J. Performance of 18 polymers in aluminum citrate colloidal dispersion gels. *SPE International Symposium on Oilfield Chemistry*; OnePetro, 1995.

(11) Sydansk, R. D.; Southwell, G. More than 12 years' experience with a successful conformance-control polymer-gel technology. *SPE Prod. Facil.* **2000**, *15* (04), 270−278.

(12) Lei, G.; Li, L.; Nasr-El-Din, H. A. New gel aggregates to improve sweep efficiency during waterflooding. *SPE Reservoir Eval. Eng.* **2011**, *14* (01), 120−128.

(13) Zhang, Z.; Zhao, L.; Cao, B. Applicability evaluation and application of hydrophobic association polymer weak gel. *Petrochem. Ind. Appl.* **2018**, *1*, 65−69.

(14) Zhu, D.; Bai, B.; Hou, J. Polymer gel systems for water management in high-temperature petroleum reservoirs: a chemical review. *Energy Fuels* **2017**, *31* (12), 13063−13087.

(15) Liu, Y.; Li, Y.; Zhang, Y.; Li, H.; Xue, B.; Wang, N.; Lu, X.; Dai, L.; Xia, H.; Xie, K. Water-alternating-weak gel technology and its application in high water cut oil reservoir in bohai oilfield. *SPE Middle East Oil and Gas Show and Conference*; OnePetro, 2019.

(16) Sheng, J. *Modern Chemical Enhanced Oil Recovery: Theory and Practice*; Gulf Professional Publishing, 2010.

(17) Han, M.; Alshehri, A. J.; Krinis, D.; Lyngra, S. State-of-the-art of in-depth fluid diversion technology: enhancing reservoir oil recovery by gel treatments. *SPE Kingdom of Saudi Arabia Annual Technical Symposium and Exhibition*; Society of Petroleum Engineers, 2014.

(18) Song, W.; Zeng, X.; Yao, H.; Li, J.; Tian, Y.; Gao, Y. *Application of a New Crosslinked Polymer Displacement Technology at Bo-19 Block in Gudao Oilfield*; Society of Petroleum Engineers, 2003.

(19) Lu, X.; Wang, W.; Wang, R.; Liu, Y.; Shan, J. C. The performance characteristics of Cr3+ polymer gel and its application analysis in bohai oilfield. *International Oil and Gas Conference and Exhibition in China*; OnePetro, 2010.

https://doi.org/10.1021/acsomega.3c10244
ACS Omega 2024, 9, 7597−7608

(20) Shi-yi, Y.; Dong, H.; Kun, M.; Man-ku, Z.; Li, W. Application of flowing gel profile control technique to complex block reservoir. *Acta Pet. Sin.* **2004**, *25* (4), 50.
(21) El-Karsani, K. S.; Al-Muntasheri, G. A.; Hussein, I. A. Polymer systems for water shutoff and profile modification: a review over the last decade. *SPE J.* **2014**, *19* (01), 135−149.
(22) Quezada, G. R.; Toro, N.; Saavedra, J.; Robles, P.; Salazar, I.; Navarra, A.; Jeldres, R. I. Molecular dynamics study of the conformation, ion adsorption, diffusion, and water structure of soluble polymers in saline solutions. *Polymers* **2021**, *13* (20), 3550.
(23) Cui, C.; Zhou, Z.; He, Z. Enhance oil recovery in low permeability reservoirs: Optimization and evaluation of ultra-high molecular weight HPAM/phenolic weak gel system. *J. Pet. Sci. Eng.* **2020**, *195*, 107908.
(24) Akbar, I.; Hongtao, Z. The opportunities and challenges of preformed particle gel in enhanced oil recovery. *Recent Innovations Chem. Eng.* **2020**, *13* (4), 290−302.
(25) Al-Ibadi, A.; Civan, F. Experimental investigation and correlation of treatment in weak and high-permeability formations by use of gel particles. *SPE Prod. Oper.* **2013**, *28* (04), 387−401.
(26) Li, Z.; Zhao, G.; Xiang, C. Synthesis and Properties of a Gel Agent with a High Salt Resistance for Use in Weak-Gel-Type Water-Based Drilling Fluid. *Arabian J. Sci. Eng.* **2022**, *47* (9), 12045−12055.
(27) Imqam, A.; Bai, B.; Al Ramadan, M.; Wei, M.; Delshad, M.; Sepehrnoori, K. Preformed particle gel extrusion through open conduits during conformance control treatments. *SPE Improved Oil Recovery Conference?*; Society of Petroleum Engineers, 2014.
(28) Qi, Y.-B.; Zheng, C.-G.; Lv, C.-Y.; Lun, Z.-M.; Ma, T. Compatibility between weak gel and microorganisms in weak gel-assisted microbial enhanced oil recovery. *J. Biosci. Bioeng.* **2018**, *126* (2), 235−240.
(29) Li, S.; Zhang, S.; Zou, Y.; Zhang, X.; Ma, X.; Wu, S.; Zhang, Z.; Sun, Z.; Liu, C. Experimental study on the feasibility of supercritical CO2-gel fracturing for stimulating shale oil reservoirs. *Eng. Fract. Mech.* **2020**, *238*, 107276.
(30) Almohsin, A.; Bai, B.; Imqam, A.; Wei, M.; Kang, W.; Delshad, M.; Sepehrnoori, K. Transport of nanogel through porous media and its resistance to water flow. *SPE Improved Oil Recovery Conference?*; Society of Petroleum Engineers, 2014.
(31) Chen, S.; Li, J.; Chen, S.; Qin, J.; Wang, G.; Yi, Y.; Zhang, L.; Wang, R.; Zhu, D. Experimental Evaluation of Combined Plugging System for CO2-Improved Oil Recovery and Storage. *Energy Fuels* **2023**, *37* (6), 4401−4412.
(32) Amir, Z.; Saaid, I. M.; Mohd Junaidi, M. U.; Wan Bakar, W. Z. Weakened PAM/PEI polymer gel for oilfield water control: Remedy with silica nanoparticles. *Gels* **2022**, *8* (5), 265.
(33) Reddy, B.; Eoff, L.; Dalrymple, E. D.; Black, K.; Brown, D.; Rietjens, M. A natural polymer-based cross-linker system for conformance gel systems. *SPE J.* **2003**, *8* (02), 99−106.
(34) Al-Muntasheri, G. A.; Nasr-El-Din, H. A.; Zitha, P. L. Gelation kinetics and performance evaluation of an organically crosslinked gel at high temperature and pressure. *SPE J.* **2008**, *13* (03), 337−345.
(35) El-Karsani, K. S.; Al-Muntasheri, G. A.; Sultan, A. S.; Hussein, I. A. Gelation of a water-shutoff gel at high pressure and high temperature: rheological investigation. *SPE J.* **2015**, *20* (05), 1103−1112.
(36) Seddiqi, K. N.; Abe, K.; Hao, H.; Mahdi, Z.; Liu, H.; Hou, J. Optimization and Performance Evaluation of a Foam Plugging Profile Control Well Selection System. *ACS Omega* **2023**, *8*, 10342−10354.

https://doi.org/10.1021/acsomega.3c10244
ACS Omega 2024, 9, 7597−7608